

SUPPLEMENTARY DATA

Section 1: Whole exome sequencing analyses for patient 1 and patient 2.

Patient genomic DNA was extracted from whole blood using the Gentra Puregene Blood kit (Qiagen, Valencia, CA). Patient genomic DNA was then sent for SNP array and whole exome sequencing. Sequence reads collected from patient genomic DNA were aligned and genotyped using the UDP's DiploidAlign pipeline. Briefly, BEAGLE software version 3 was used to generate a phased and imputed Variant Call Format (VCF) file from SNP chip data of the parents and offspring and 1000 Genomes HapMap data.¹ The VCF file was then used by vcf2diploid version 0.2.3 to modify the human reference (hg19) and create a maternal reference and a paternal reference, which were concatenated together to generate a parental reference.² Patient short reads were aligned with Novoalign version 2.08.03 (<http://www.novocraft.com/main/downloadpage.php>) to each of the three reference sequences and were lifted back over to the standard human reference using a custom extension of Picard Liftover Java class. Bam files were recalibrated and genotyped by HaplotypeCaller and GenotypeGVCFs according to GATK Best Practices using GATK v2.5-2 (<http://www.broadinstitute.org/gatk/>).³

The VCF files were annotated relative to RefSeq transcripts using SnpEff.⁴ Each variant was filtered for rarity in the population, segregation with disease, protein deleteriousness, and quality. We defined a variant as rare if it had an allele frequency of <2% in the UDP founders cohort, African and European populations in the 1000 Genomes Project (version hg19_v3_20101123), and African American and European American populations in the Exome Sequencing Project (ESP6500SI-V2). If any one of these populations had fewer than 100 genotyped individuals at the genomic position of the variant, then that population's allele frequency was disregarded for filtration, with exception to the UDP founders cohort for which an allele frequency of <5% at a position that had 50-99 individuals genotyped individuals was also acceptable. Only rare variants that segregated with disease according to an autosomal recessive, *de novo* dominant, or X-linked recessive inheritance models were kept. We then excluded biallelic variants that (excluding the affected individuals of each family) occurred in homozygosity more than once in the UDP founders cohort and *de novo* variants that (excluding the affected individuals of each family) occurred more than twice in the UDP founders cohort. From the remaining variants, we selected those annotated as nonsynonymous, frame shift, premature stop, loss of start codon, loss of stop codon, or splicing mutations.

To test for copy number variants, Omni Express 1.1B for patient 1 and Omni Express 1.2 for patient 2 (hg19) SNP arrays were run on genomic DNA from all family members as described.⁵ For both families, deletion BED files were generated with PENNCNV using the minimum SNP threshold of five (Table S-1).⁶ Exomic variants located within the regions of the family's deletion BED file that passed the filters described above and segregated appropriately were considered. Since patient 1 had an available sibling, a recessive segregation BED file was generated. All autosomal recessive exomic variants were required to pass filtration and fall within the regions delineated in the recessive segregation BED file.⁵

Table S-1. Copy number variations detected in the proband.

UDP_5185					UDP_6399				
CNV region (hg19)	Copy number	Parent of origin	No. of genes within region	Genes	CNV region (hg19)	Copy number	Parent of origin	No. of genes within region	Genes
chr1:149039930-149201987	1	Maternal	0	-	chr4:33355067-33411555	1	Maternal	0	-
chr3:2902492-2906446	1	Paternal	1	CNTN4	chr8:3996630-4005469	1	Maternal	0	-
chr3:175893082-175907342	1	Maternal	0	-	chr8:75602527-71676477	1	Paternal	1	XKR9
chr5:151514956-151518810	1	Paternal	1	AK001582, intronic	chr9:570428-626231	1	Maternal	1	KANK1, intronic
chr6:31221485-31228972	1	Paternal	0	-	chr11:104918425-104936068	1	Maternal	1	CASP1, intronic
chr6:67017494-67047294	1	Maternal	0	-	chr19:54720950-54749154	1	Maternal	2	LILRB3, LILRA6
chr8:137682484-137857327	1	Maternal	0	-	chr9:11224194-11531715	3	Paternal	0	-
chr9:8009428-8014674	1	Paternal	0	-	chr11:27248923-27276563	3	Paternal	0	-
chr10:42725663-42827951	1	Maternal	1	LOC441666	chr15:43893272-44049665	3	Paternal	5	STRC, CATSPER2, CKMT1A, CATSPER2P1, PDIA3
chr10:82879719-82890180	1	Maternal	0	-	chr17:44164016-44583060	3	Paternal	5	KANSL1, KNSL1-AS1, ARL17A, ARL17B, LRRC37A
chr2:34699812-34717799	3	Neither	0	-	chr19:43557716-43767348	3	Maternal	3	PSG2, PSG4, PSG5
chr5:139931633-139931740	3	Neither	1	SRA1	chr21:21299953-21336134	3	Maternal	0	-

The variants that passed filtration for each mode of inheritance were submitted to Exomiser v4.0.1 (http://ftp.sanger.ac.uk/pub/resources/software/exomiser/downloads/exomiser/old_versions). All the variants were recombined, ranked on their Exomiser score for interpretation, and BAM file curated using the Integrative Genome Viewer (<https://www.broadinstitute.org/igv/home>) to assess the quality of the variant's alignment and genotype call in all family members.⁷ Variants with an Exomiser score ≥ 0.1 were Sanger sequenced to validate (Table S-2 and S-3).

Exomiser is a variant prioritization algorithm that uses Human Phenotype Ontology descriptors⁸ and the OwlSim (v1. 5) algorithm to compare patient phenotypes to known human diseases,^{9,10} mouse phenotype data (Mouse Genome Informatics and the Sanger Mouse Portal : <http://www.sanger.ac.uk/mouseportal>),¹¹ and zebrafish phenotype data.¹²⁻¹⁶ Exomiser also performs a network analysis using a random walk algorithm to compare phenotype data for neighboring proteins in the network and phenotype data for proteins with similar function to the patient's phenotype.¹⁷ The Exomiser algorithm combines this phenotype analysis with a variant analysis that is based on predicted deleteriousness (Polyphen2, MutationTaster, and SIFT) and allele frequencies (1000 Genomes and Exome Sequencing Project). The score on which variants are prioritized is a combination of phenotype score and variant score as determined by logistic regression on a training set of 10,000 HGMD disease variants and 10,000 benign variants from the 1000 Genomes.¹²

References

1. Rozowsky J, Abyzov A, Wang J, et al. AlleleSeq: analysis of allele-specific expression and binding in a network framework. *Mol Syst Biol*. 2011;7:522 doi: 10.1038/msb.2011.54.
2. Browning BL, Browning SR. A unified approach to genotype imputation and haplotype-phase inference for large data sets of trios and unrelated individuals. *Am J Hum Genet*. 2009;84(2):210-23. doi: 10.1016/j.ajhg.2009.01.005.
3. McKenna A, Hanna M, Banks E, et al. The Genome Analysis Toolkit: a MapReduce framework for analyzing next-generation DNA sequencing data. *Genome Res*. 2010;20(9):1297-303. doi: 10.1101/gr.107524.110. .
4. Cingolani P, Platts A, Wang le L, et al. A program for annotating and predicting the effects of single nucleotide polymorphisms, SnpEff: SNPs in the genome of *Drosophila melanogaster* strain w1118; iso-2; iso-3. *Fly (Austin)*. 2012;6(2):80-92. doi: 10.4161/fly.19695.
5. Markello TC, Han T, Carlson-Donohoe H, et al. Recombination mapping using Boolean logic and high-density SNP genotyping for exome sequence filtering. *Mol Genet Metab*. 2012;105(3):382-9. doi: 10.1016/j.ymgme.2011.12.014.
6. Wang K, Li M, Hadley D, et al. PennCNV: an integrated hidden Markov model designed for high-resolution copy number variation detection in whole-genome SNP genotyping data. *Genome Res*. 2007;17(11):1665-74.
7. Thorvaldsdottir H, Robinson JT, Mesirov JP. Integrative Genomics Viewer (IGV): high-performance genomics data visualization and exploration. *Brief Bioinform*. 2013;14(2):178-92. doi: 10.1093/bib/bbs017.
8. Robinson PN, Köhler S, Bauer S, Seelow D, Horn D, Mundlos S. The Human Phenotype Ontology: a tool for annotating and analyzing human hereditary disease. *Am J Hum Genet*. 2008;83(5):610-5. doi: 10.1016/j.ajhg.2008.09.017. .
9. Amberger J, Bocchini C, Hamosh A. A new face and new challenges for Online Mendelian Inheritance in Man (OMIM(R)). *Hum Mutat*. 2011;32(5):564-7. doi: 10.1002/humu.21466. .
10. Maiella S, Rath A, Angin C, Mousson F, Kremp O. [Orphanet and its consortium: where to find expert-validated information on rare diseases]. *Rev Neurol (Paris)*. 2013;169(Suppl 1):S3-8. doi: 10.1016/S0035-3787(13)70052-3.
11. Bult CJ, Eppig JT, Blake JA, Kadin JA, Richardson JE. The mouse genome database: genotypes, phenotypes, and models of human disease. *Nucleic Acids Res*. 2013;41(Database issue):D885-91. doi: 10.1093/nar/gks1115. .
12. Bone WP, Washington NL, Buske OJ, et al. Computational evaluation of exome sequence data using human and model organism phenotypes improves diagnostic efficiency. [Unpublished].
13. Gkoutos GV, Green EC, Mallon AM, Hancock JM, Davidson D. Using ontologies to describe mouse phenotypes. *Genome Biol*. 2005;6(1):R8.
14. Mungall CJ, Gkoutos GV, Smith CL, Haendel MA, Lewis SE, Ashburner M. Integrating phenotype ontologies across multiple species. *Genome Biol*. 2010;11(1):R2. doi: 10.1186/gb-2010-11-1-r2.
15. Robinson PN, Köhler S, Oellrich A, et al. Improved exome prioritization of disease genes through cross-species phenotype comparison. *Genome Res*. 2014;24(2):340-8. doi: 10.1101/gr.160325.113.
16. Van Slyke CE, Bradford YM, Westerfield M, Haendel MA. The zebrafish anatomy and stage ontologies: representing the anatomy and development of *Danio rerio*. *J Biomed Semantics*. 2014;5(1):12. doi: 10.1186/2041-1480-5-12.
17. Köhler S, Bauer S, Horn D, Robinson PN. Walking the interactome for prioritization of candidate disease genes. *Am J Hum Genet*. 2008;82(4):949-58. doi: 10.1016/j.ajhg.2008.02.013.

Table S-2. Exome variants meeting rarity, predicted deleteriousness, and phenotype match requirements and segregating with disease for patient 1.

Gene	Chr	Position (hg19)	Reference allele	Variant allele	GT	Transcript	cDNA change	Protein change	dbSNP	Phenotype score	Variant score	Exomiser score	IGV	S	Seg
PLA2G6	22	38528965	G	A	Het	NM_003560	c.950C>T	p.Gly317Val	-	0.71	0.98	0.96*		GT	Y
PLA2G6	22	38539295	-	**	Het	NM_003560	c.426-?_1077+?dup	p.Lys360Leufs*22	-	0.71	0.98	0.96*		***	Y
SGPP1	14	64194659	A	G	Het	NM_030791	c.4T>C	p.Ser2Pro	-	0.6	1	0.89	LC	AA	N
P4HB	17	79818224	T	A	Het	NM_000918	c.124A>T	p.Lys42*	-	0.54	0.95	0.73	LC	TT	N
P4HB	17	79818232	G	T	Het	NM_000918	c.116C>A	p.Ala39Glu	-	0.54	0.95	0.73	LC	GG	N
ABL1	9	133710914	T	C	Het	NM_007313	c.137-18537T>C	intron 1	-	0.57	0.9	0.72	LC	TT	N
ABL1	9	133710919	C	T	Het	NM_007313	c.137-18532C>G	intron 1	-	0.57	0.9	0.72	LC	CC	N
CACNA2D1	7	82072718	C	G	Het	NM_000722	c.58G>C	p.Gly20Arg	-	0.43	1	0.6	LC	CC	N
DDX54; RITA1	12	113623185	T	G	Het	NM_00111322	c.72A>C	p.Lys24Asn	-	0.45	0.98	0.6	LC	TT	N
MATR3	5	138651879	-	GCTGGAAATGGA	Het	NM_199189	c.1129+2_1129+3ins GCTGGAAATGGA	intron 8	-	0.9	0.44	0.39	Fail	-	N
MATR3	5	138654722	-	AAACCT	Het	NM_199189	c.1434_1434+1insA AACT	p.Lys479_Pro480dup	-	0.9	0.44	0.39	Fail	-	N
MATR3	5	138654722	-	GGACAAGATCGA GGAACCTGATCA AGAAAACGAAGC AGCGTTGGAAAA TGGAAATTA	Het	NM_199189	c.2148+2insGGACAA GATGGAGGAACTTG ATCAAGAAAAACGAA GCAGCGTTGAAAA TGGAAATTA	intron 15	-	0.9	0.44	0.39	Fail	-	N
EYPL	17	74018007	G	C	Het	NM_001988	c.748C>G	p.Leu250Val	-	0.34	0.99	0.35	LC	GG	N
EYPL	17	74018016	G	C	Het	NM_001988	c.739C>G	p.Arg247Gly	-	0.34	0.99	0.35	LC	GG	N
MTMR7	8	17218784	C	T	Het	NM_004686	c.311-1G>A	intron 3	-	0.38	0.9	0.26	Pass	CC	N
CPEB3	10	93999419	G	A	Het	NM_001178137	c.689C>T	p.Arg230Val	-	0.37	0.89	0.22	LC	GG	N
CPEB3	10	93999428	G	C	Het	NM_001178137	c.680C>G	p.Arg227Gly	-	0.37	0.89	0.22	LC	GG	N
HECW1	7	43540840	G	A	Hom	NM_001287059	c.3550G>A	p.Val1150Ile	rs117557838	0.4	0.78	0.12	Pass	AA	Y
HECW1	7	43540841	T	C	Hom	NM_001287059	c.3551T>C	p.Val1150Ala	rs116945469	0.4	0.78	0.12	Pass	AA	Y

Abbreviations: Chr, chromosome; GT, genotype; Het, heterozygous; Hom, homozygous; S, Sanger sequencing result in patient; Seg, segregates with disease in family; LC, low coverage from exome data

* Variants originally did not pass our exome filters because the large duplication was not identified by exome analysis. Therefore the second variant did not pass as only one of a set of compound heterozygous mutations.

** Due to low complexity of the area around the genomic breakpoint this could not be Sanger validated.

*** The complete duplication of exon 4-7 was confirmed on cDNA level (see figure 1 of the main manuscript).

Table S-3. Exome variants meeting rarity, predicted deleteriousness, and phenotype match requirements and segregating with disease for patient 2.

Gene	Chr	Position (hg19)	Reference allele	Variant allele	GT	Transcript	cDNA change	Protein change	dbSNP	Phenotype score	Variant score	Exomiser score	IGV	S	Seg
PLA2G6; BAIAP2L2	22	38508565	C	T	Het	NM_003560	c.2222G>A	p.Arg741Gln	rs121908686	0.6	1	0.89	Pass	CT	Y
PLA2G6	22	38539112	C	T	Het	NM_003560	c.609G>A	(p.Gln203Gln)*	-	0.6	1	0.89	Pass	CT	Y
TTN; MIR548N	2	179395813	C	T	Het	NM_001267550	c.105529G>A	p.Val35177Met	rs55865274	0.49	1	0.73	Pass	CT	Y
TTN; MIR548N	2	179418415	T	A	Het	NM_001267550	c.89317A>T	p.Ile29773Leu	rs77853750	0.49	1	0.73	Pass	TA	Y
TTN; MIR548N	2	179428373	C	T	Het	NM_001267550	c.8248G>A	p.Asp27496Asn	-	0.49	1	0.73	Pass	CT	Y
TTN; MIR548N	2	179447008	G	A	Het	NM_001267550	c.66160+15C>T	intron 315	-	0.49	1	0.73	Pass	GA	Y
TTN	2	179582063	A	T	Het	NM_001267550	c.25398T>A	p.Asp8466Glu	rs72648986	0.49	1	0.73	Pass	AT	Y
TTN	2	179588996	C	T	Het	NM_001267550	c.21106G>A	p.Asp7036Asn	rs72648962	0.49	1	0.73	Pass	CT	Y
TTN	2	179593449	T	C	Het	NM_001267550	c.19204A>G	p.Met6402Val	rs72648954	0.49	1	0.73	Pass	TC	Y
TTN	2	179593761	T	C	Het	NM_001267550	c.19004A>G	p.Asp6335Gly	rs72648951	0.49	1	0.73	Pass	TC	Y
TTN	2	179595528	T	C	Het	NM_001267550	c.17741-9A>G	intron 61	rs72648944	0.49	1	0.73	Pass	TC	Y
TTN	2	179598124	C	G	Het	NM_001267550	c.15896G>C	p.Arg5299Thr	-	0.49	1	0.73	Pass	CG	Y
TTN	2	179606241	G	C	Het	NM_001267550	c.11719C>G	p.Leu3907Val	rs55853696	0.49	1	0.73	Pass	GC	Y
TTN	2	179659118	G	A	Het	NM_001267550	c.1398+8C>T	intron 8	rs72647848	0.49	1	0.73	Pass	GA	Y
TTN	2	179659891	C	T	Het	NM_001267550	c.1003G>A	p.Val335Met	rs72647846	0.49	1	0.73	Pass	CT	Y
HLA-DRB1	6	32552133	-	ATGT	Het	NM_002124	c.123insATGT	p.Arg42Tyrfs*22	-	0.51	0.95	0.67	Fail	-	N
HLA-DRB1	6	32552135	T	A	Het	NM_002124	c.121A>T	p.Lys41*	-	0.51	0.95	0.67	Fail	TT	N
HLA-DRB1	6	32552159	T	C	Het	NM_002124	c.101-4A>G	intron 1	-	0.51	0.95	0.67	Fail	CC	N
DVL3	3	183885832	A	G	Hom	NM_004423	c.1477A>G	p.Ile493Val	-	0.42	1	0.57	Pass	GG	Y
GJB2	13	20763341	C	T	Het	NM_004004	c.380G>A	p.Arg127His	rs111033196	0.51	0.88	0.53	Pass	CT	Y
GJB2	13	20763650	C	T	Het	NM_004004	c.71G>A	p.Trp24*	rs104894396	0.51	0.88	0.53	Pass	CT	Y
IRS4; LOC101928358	X	107977323	C	A	Het	NM_003604	c.2252G>T	p.Ser751Ile	-	0.4	0.99	0.5	Fail	CC	N

Abbreviations: Chr, chromosome; GT, genotype; Het, heterozygous; Hom, homozygous; S, Sanger sequencing result in patient; Seg, segregates with disease in family; LC, low coverage from exome data

* This variant encodes a synonymous mutation at the last base of exon 4 that weakens the splice donor site. An alternative splice donor site 9bp upstream is the stronger one leading to a 3 amino acid deletion p.201_203delVLQ (see figure 1 of the main manuscript).

Table S-3. Exome variants meeting rarity, predicted deleteriousness, and phenotype match requirements and segregating with disease for patient 2 (continued).

Gene	Chr	Position (hg19)	Reference allele	Variant allele	GT	Transcript	cDNA change	Protein change	dbSNP	Phenotype score	Variant score	Exomiser score	IGV	S	Seg
LILRB2	19	54779797	G	A	Het	NM_005874	c.1650+8C>T	intron 13	rs73938622	0.39	0.96	0.4	Pass	GA	Y
LILRB2; MIR4752	19	54782393	T	G	Het	NM_005874	c.979A>C	p.Ile327Leu	rs116027944	0.39	0.96	0.4	Fail	TG	N
LILRB2; MIR4752	19	54782395	A	G	Het	NM_005874	c.977T>C	p.Phe326Ser	rs7246737	0.39	0.96	0.4	Fail	AG	N
LILRB2; MIR4752	19	54782401	G	C	Het	NM_005874	c.971C>G	p.Thr324Arg	rs7247055	0.39	0.96	0.4	Fail	GC	N
LILRB2; MIR4752	19	54782805	G	T	Het	NM_005874	c.817C>A	p.Gln273Lys	rs201709101	0.39	0.96	0.4	Fail	GC	N
LILRB2; MIR4752	19	54782808	G	A	Het	NM_005874	c.814C>T	p.Pro272Ser	rs199893740	0.39	0.96	0.4	Fail	GG	N
LILRB2; MIR4752	19	54782813	C	T	Het	NM_005874	c.809G>A	p.Arg270Gln	rs141001610	0.39	0.96	0.4	Fail	CC	N
LILRB2; MIR4752	19	54782819	G	T	Het	NM_005874	c.803C>A	p.Pro268His	rs202225109	0.39	0.96	0.4	Fail	GG	N
LILRB2; MIR4752	19	54782835	C	T	Het	NM_005874	c.787G>A	p.Asp263Asn	rs201144349	0.39	0.96	0.4	Fail	CC	N
LILRB2; MIR4752	19	54782864	C	T	Het	NM_005874	c.758G>A	p.Arg253Lys	rs201954016	0.39	0.95	0.4	Fail	CC	N
LILRB2; MIR4752	19	54782885	A	C	Het	NM_005874	c.737T>G	p.Val246Gly	-	0.39	0.96	0.4	Fail	AA	N
LILRB2; MIR4752	19	54782903	C	T	Het	NM_005874	c.719G>A	p.Ser240Asn	-	0.39	0.96	0.4	Fail	CC	N
LILRB2; MIR4752	19	54782922	C	T	Het	NM_005874	c.700G>A	p.Val234Ile	-	0.39	0.96	0.4	Fail	CC	N
LILRB2; MIR4752	19	54782973	G	-	Het	NM_005874	c.659-10delC	intron 5	-	0.39	0.96	0.4	Pass	GG	N
LILRB2; MIR4752	19	54782977	C	G	Het	NM_005874	c.659-14G>C	intron 5	rs199662056	0.39	0.96	0.4	Pass	CC	N
LILRB2; MIR4752	19	54783522	C	T	Het	NM_005874	c.356-20G>A	intron 4	rs200913010	0.39	0.96	0.4	Pass	CT	N
LILRB2; MIR4752	19	54784122	T	C	Het	NM_005874	c.67A>G	p.Thr23Ala	rs45557835	0.39	0.96	0.4	Pass	TC	N
LILRB2; MIR4752	19	54784300	T	-	Het	NM_005874	c.34+18delA	intron 2	rs200095982	0.39	0.96	0.4	Pass	T-	Y
LILRB2; MIR4752	19	54784302	T	A	Het	NM_005874	c.34+16A>T	intron 2	rs183405168	0.39	0.96	0.4	Pass	TAC**	Y
LILRB2	19	54778582	TT	-	Het	NM_005874	c.1751_1752delAA	p.Glu584Alafs*4	-	0.37	0.95	0.32	Fail	TT/--	Y
LILRB2	19	54778587	T	-	Het	NM_005874	c.1747delA	p.Arg583Glyfs*68	-	0.37	0.95	0.32	Fail	TA/T-	Y
ADRA2A	10	112838506	C	G	Het	NM_000681	c.752C>G	p.Pro251Arg	-	0.47	1	0.21	Fail	CG	N
CLN3	16	28493437	C	T	Het	NM_001042432	c.1045G>A	p.Ala349Thr	-	0.42	0.72	0.09	Pass	CT	Y
CLN3	16	28499044	T	C	Het	NM_001042432	c.313A>G	p.Ile105Val	rs11552531	0.42	0.72	0.09	Pass	TC	Y

Abbreviations: Chr, chromosome; GT, genotype; Het, heterozygous; Hom, homozygous; S, Sanger sequencing result in patient; Seg, segregates with disease in family; LC, low coverage from exome data

** Through single strand sequencing 3 alleles were identified, the predicted AT and an additional G in all family members. Probably a second position in the genome closely matches this region, like another LILRB-gene, leading to the apparent additional allele.

Section 2: Supplementary figures and tables

Table S-4. Primers used for PCR amplification and Sanger sequencing

Patient	Mutation	Exon	Forward primer 5' to 3'	Reverse primer 5' to 3'
1	c.950G>T	7	TCAGAGCAGAAGTGGCAGTG	TCAGAGCAGAAGTGGCAGTG
	c.426-1077dup	4 - 7	NA*	NA*
2	c.609G>A	4	GTCCACACTAGGGCTGGG	GCTCAGCCTGACTCGAAAG
	c.2222G>A	16	GAAAAGGGCTGGGAGGGAA	GGAGAACGAGGAGGGCTG
3	c.1799G>A	13	GTGTGAATTGTGGGGAAAGG	GATGGCAAGTGCACGACTC
	c.2221C>T	16	CTGACTCGAAAGAGCCTGG	GGGAACAGAGCAGACCCTTG

* The duplication of exon 4 - 7 was confirmed by multiplex ligation-dependent probe amplification.

Figure S-1. Protein expression in Patient 1 (P1) with and without overexpression of iPLA2VIA-1 compared to control (C).

Analysis of protein expression by western blot. GAPDH protein served as loading control. Similar overexpression levels were obtained for iPLA2VIA-1 and iPLA2VIA-2 in all three patients (data not shown).

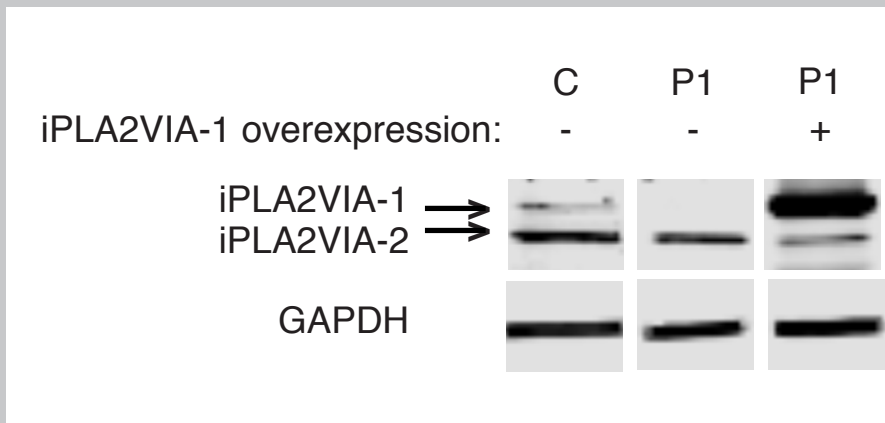


Figure S-2. Glycosylation analysis using lectins MAL-II, SNA, PNA and sWGA

Laser-scanning microscope images (A) and quantification of the signal intensity (B) of the lectin stain against alpha-2,3-sialic acid (SNA) and alpha-2,6-sialic acid (MAL-II) and terminal galactose (PNA) in cultured skin fibroblasts of a control before and after neuraminidase treatment and in the three patients without (-) and with overexpression of iPLA2VIA-1 (1) or iPLA2VIA-2 (2). After neuraminidase treatment the signals of MAL-II and SNA decrease 2-fold whereas the signal for PNA increases 6-fold. In the patients the signals for MAL-II and SNA decrease as well but the increase in PNA intensity is minimal, suggesting a global defect in glycosylation versus a sialylation specific defect. The signal intensity for sWGA (terminal GlcNAc) shows a similar pattern as the lectins against sialylation (C). Error bars represent the standard error of the mean.

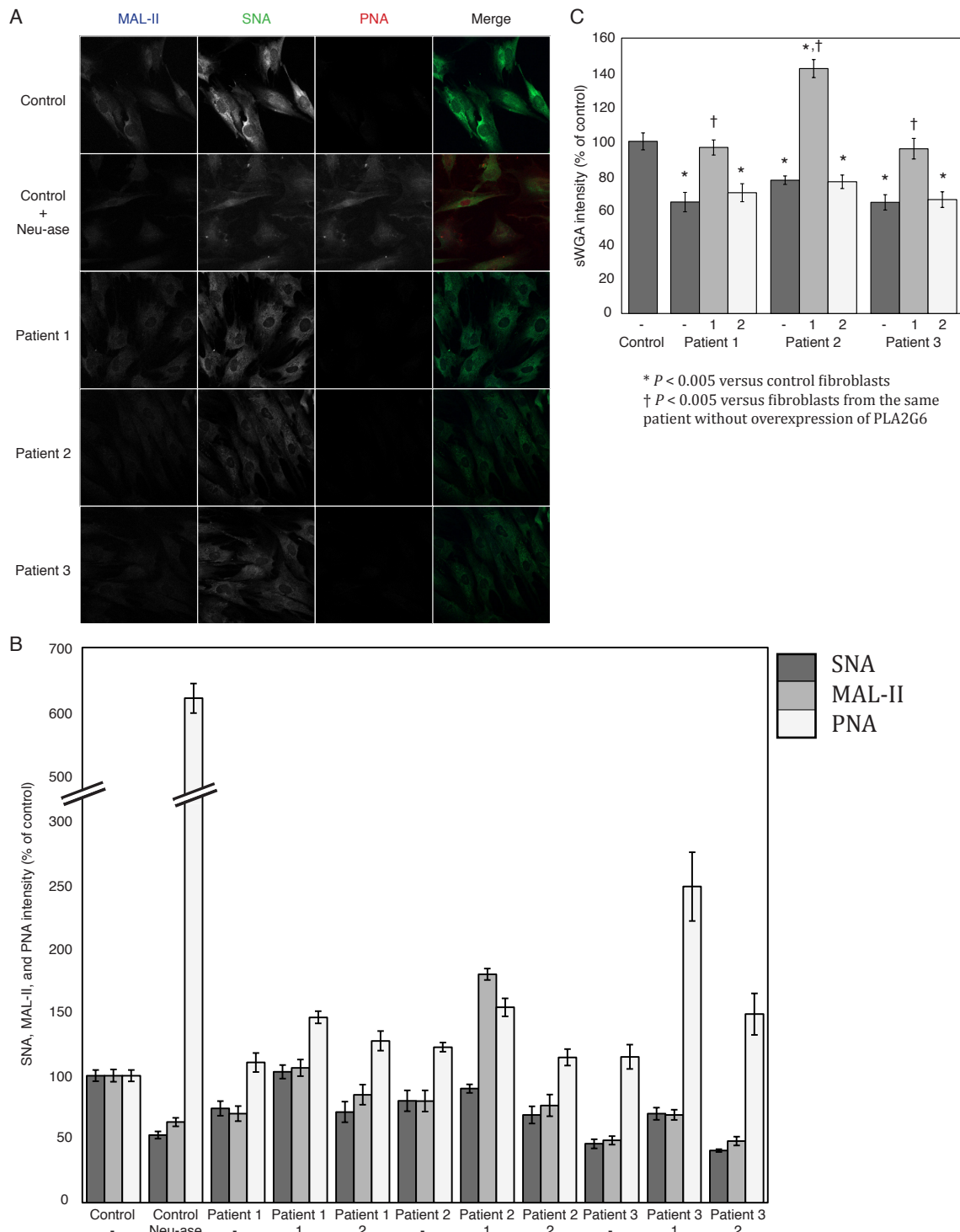


Figure S-3. Laser-scanning microscope images of the lectin stain against alpha-2,3-sialic acid (SNA) and alpha-2,6-sialic acid (MAL-II) in cultured skin fibroblasts of patient 1.

Compared to control fibroblasts. Overexpression of iPLA2VIA-1 in fibroblasts from patient 1 rescued the signal of both types of sialylation, whereas overexpression of iPLA2VIA-2 minimally improved the MAL-II and SNA intensity. Patient 2 and patient 3 had similar SNA and MAL-II profiles (data not shown).

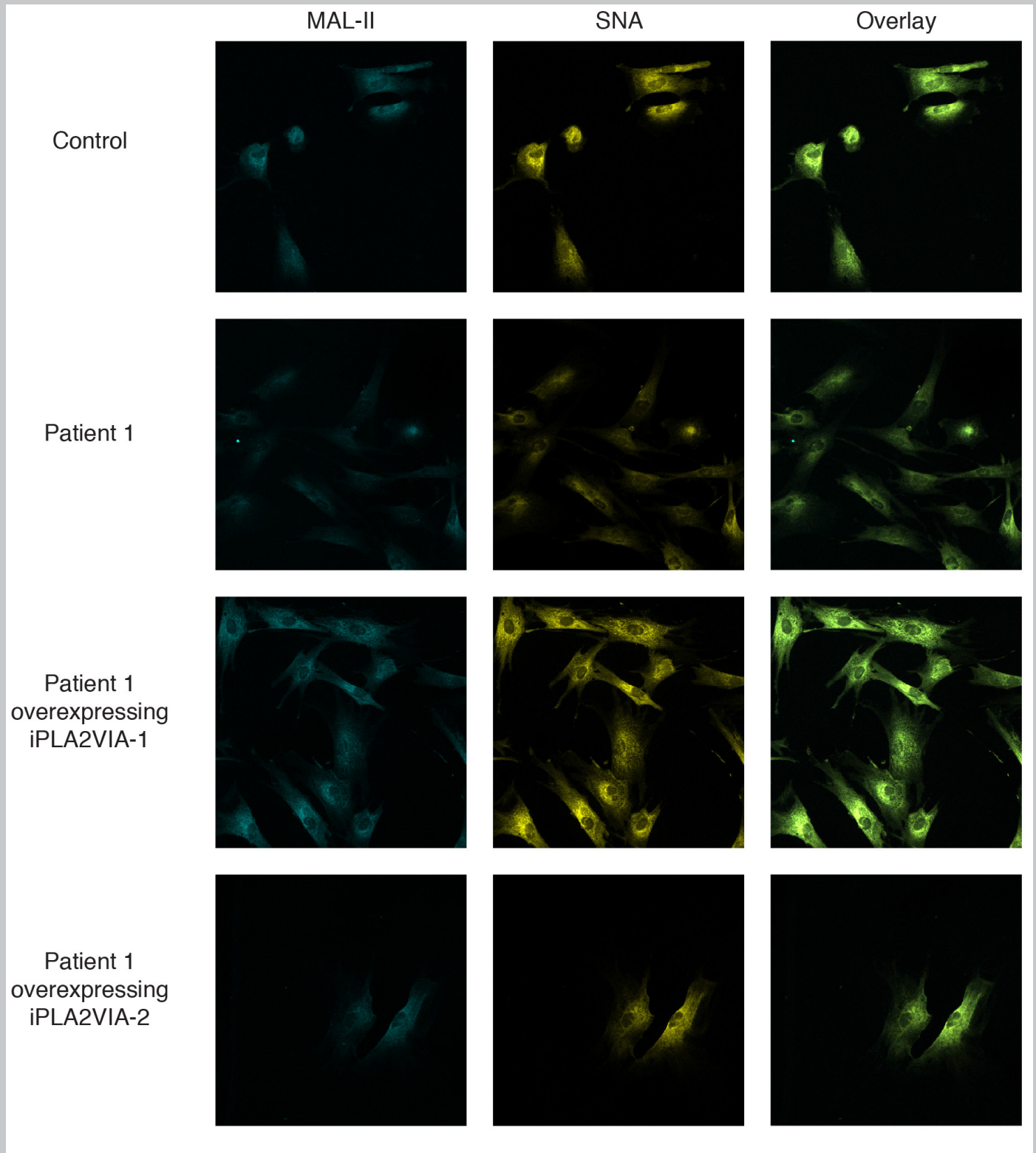


Figure S-4. Laser-scanning microscope images of the lectin stain against terminal GlcNAc (s-WGA) in cultured skin fibroblasts.

Compared to control fibroblasts, the intensity of s-WGA is significantly reduced in fibroblasts from all three patients. Overexpression of iPLA2VIA-1 rescued the signal of s-WGA, whereas overexpression of iPLA2VIA-2 minimally improved the s-WGA signal.

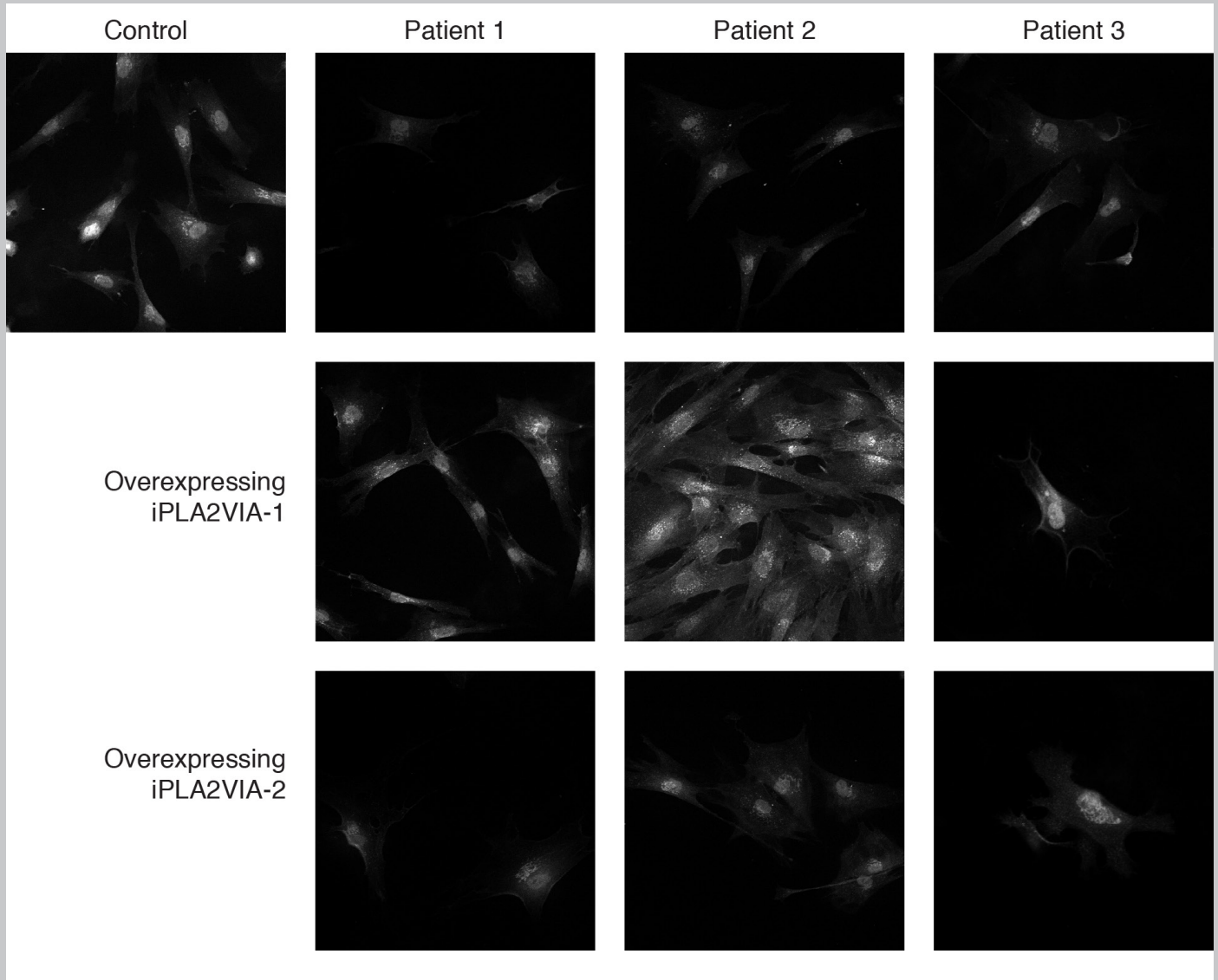


Figure S-5. Laser-scanning microscope images of the Golgi stain using anti-Golgin-97 in cultured skin fibroblasts.

Compared to control fibroblasts, the Golgi in all three patients are smaller in area and have a more round compact morphology. Overexpression of iPLA2VIA-1 rescued the Golgi morphology, whereas overexpression of iPLA2VIA-2 rescued neither Golgi size nor morphology.

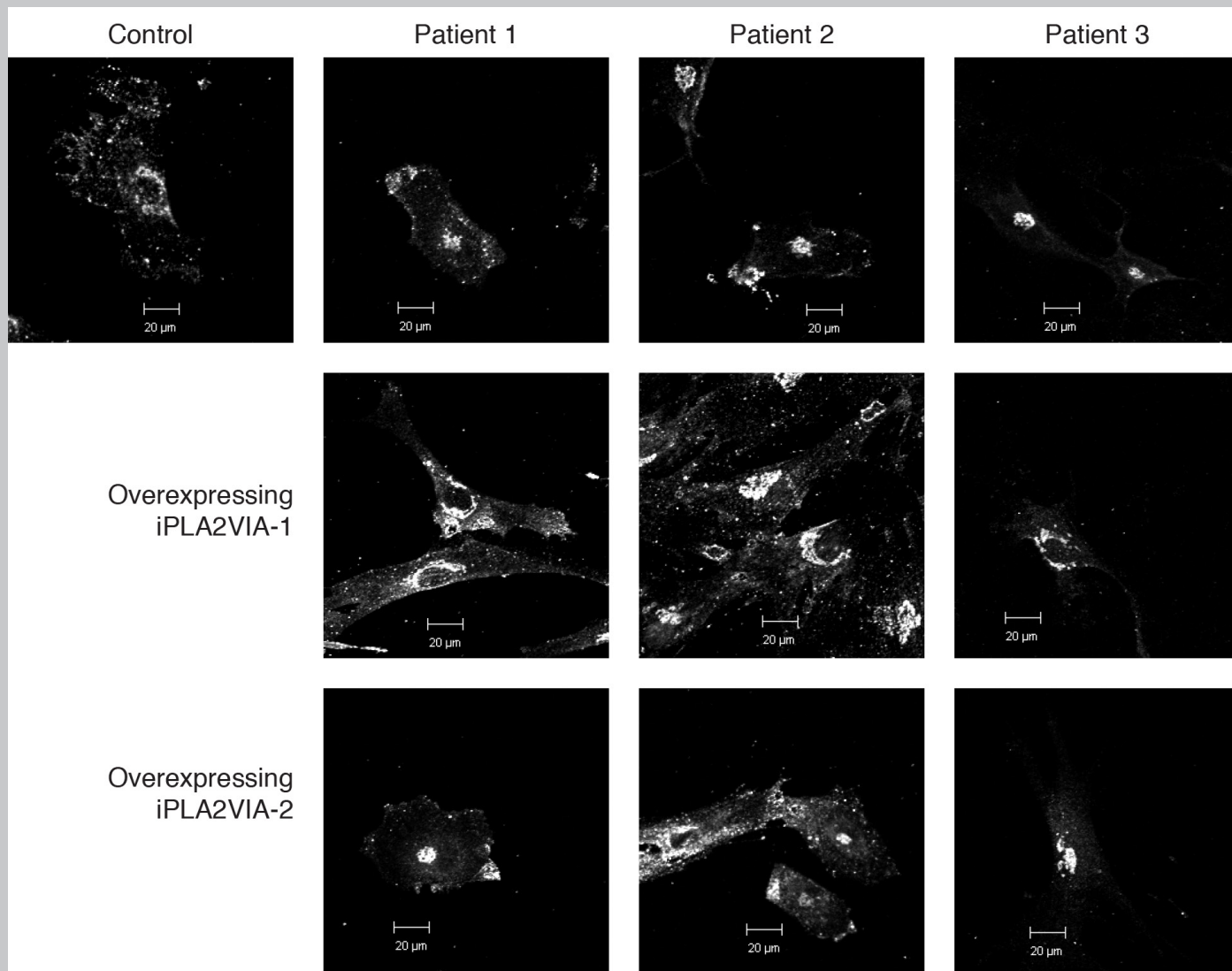


Figure S-6. Overlay of CSF O-glycan profiles of control (blue) and patient 2 (red).

Overall O-glycan levels are reduced in CSF from patient 2; particularly both monosialylated core 2 at m/z 1344 and disialylated core 2 at m/z 1705 are significantly lower in this patient compared to the control CSF. All three patients had similar profiles showing a mild general reduction of O-linked glycans in their CSF.

